Rotation-induced vibrational mixing in $\tilde{X}\,^1A_1$ formaldehyde: Non-negligible dynamical consequences of rotation

H. L. Dai, C. L. Korpa, J. L. Kinsey, and R. W. Field

Citation: The Journal of Chemical Physics **82**, 1688 (1985); doi: 10.1063/1.448401
View online: https://doi.org/10.1063/1.448401
View Table of Contents: http://aip.scitation.org/toc/jcp/82/4
Published by the American Institute of Physics

Rotation-induced vibrational mixing in $\tilde{X}\,^1A_1$ formaldehyde: Non–negligible dynamical consequences of rotation

H. L. Dai,[a] C. L. Korpa,[b] J. L. Kinsey, and R. W. Field[c]
Department of Chemistry, Massachusetts Institute of Technology, Cambridge, Massachusetts 02139

(Received 17 July 1984; accepted 29 October 1984)

Individual rotation-vibration levels of the formaldehyde $\tilde{X}\,^1A_1$ state with $7400 < E_{vib} < 8600$ cm^{-1} have been examined by the stimulated emission pumping (SEP) technique. At low values of the rotational quantum number ($J \leq 3$), the SEP spectra were simple. The only vibrational levels which appeared in the spectra were those expected either to have large Franck–Condon overlap with the $\tilde{A}\ 4^1$ level or to have appreciable Fermi resonance with a nearby Franck–Condon allowed level. At higher J and K_a values, the spectra rapidly became more complex and the observed level densities at $J \approx 10$, $K_a \approx 2$ were several times larger than the known total density of vibrational levels. This increase in the density of spectrally accessible vibrational levels was a result of rotation-induced mixing of the anharmonic vibrational basis functions (Coriolis coupling) which compromised the "goodness" of both vibrational and K_a quantum numbers. Coriolis matrix elements computed in a harmonic normal mode basis set qualitatively confirmed the importance of rotation-vibration mixing. The failure to obtain quantitative agreement is attributed to anharmonic effects. The rotation-dependent vibrational mixing effects observed in the SEP spectra indicate the importance of rotation in intramolecular vibrational dynamics and mode-selective vibrational excitation. Rotation significantly diminishes the structural differences (manifest in Franck–Condon factors, rotational constants, electric dipole moments) between rotationless vibrational levels and promotes an averaging of the character of near degenerate vibrational levels together with a partial destruction of the K_a rotational quantum number. This means that the onset of the quasicontinuum in infrared multiphoton dissociation and the inhomogeneous widths of high overtone bands would be very different for excitation out of a single low vs high J level.

I. INTRODUCTION

The idea that state-selective laser-excitation schemes might allow detailed control over chemical bond forming and breaking processes has stimulated an enormous amount of research and even more controversy. Intramolecular vibrational randomization (IVR) appears to limit the efficacy of mode- or bond-selective excitation schemes to chemically uninteresting low levels of vibrational energy.

However, a detailed understanding of IVR at the level of individual rotation-vibration eigenstates is lacking. Eigenstates are stationary and do not evolve in time. Moreover, many eigenstates have structure-related "names" in the sense that, when a spectrum is assigned, each eigenstate becomes labeled by a complete set of good and "almost good" quantum numbers. These names are not capricious; they are deduced from spectral patterns that would be evident to any trained spectroscopist. The stationary nature of the named levels implies chemically significant structural differences between neighboring vibrational levels. It is reasonable to expect *level*-specific behavior from assignable levels and to associate IVR with the *intrinsic* unassignability of a group of levels.[1] In this view, the onset of IVR would be signalled by a degradation of the structural differences between eigenstates upon which the spectral assignment process depends.

The most significant aspect of the H_2CO $\tilde{A}\,^1A_2$–$\tilde{X}\,^1A_1$ spectra reported here is that a modest amount of rotational excitation $J \simeq 10$, $K_a \simeq 2$ results in a nearly complete destruction of $\tilde{X}$ state normal mode vibrational and K_a rotational quantum numbers, even though these almost good quantum numbers reflect profound structural and spectroscopic level-to-level differences for $J \leqslant 3$, $K_a \leqslant 1$ in the region $5000 < E_{vib} < 9500$ cm^{-1}.[1] The energy onset of IVR in H_2CO is thus strongly rotation dependent. At high levels of vibrational excitation, low J levels that are spectroscopically distinguishable and vibrationally well organized, coexist with unassignable vibrationally disorganized higher J levels.

Much of molecular spectroscopy rests on a perturbation theoretic approach, with a partitioning of the molecular Hamiltonian into a zero-order term H^0 and a perturbation term H'. Our point of departure for discussing formaldehyde is a zero-order picture of the molecule as a

[a] Present address: Department of Chemistry, University of Pennsylvania, Philadelphia, PA 19104.
[b] Present address: Department of Physics, Massachusetts Institute of Technology, Cambridge, MA 02139.
[c] Address all correspondence to: Department of Chemistry, 6-219, Massachusetts Institute of Technology, Cambridge, Massachusetts 02139.

 0021-9606/85/041688-14$02.10

collection of six ($3N - 6$) independent vibrational modes (normal or local) with the rotational structure of a rigid asymmetric top. This factored zero-order basis function is

$$|\mathbf{v}, J, \tau, M\rangle^0 = \prod_{i=1}^{3N-6} |v_i\rangle |J\tau M\rangle, \quad (1)$$

where τ is the quantum number which orders the same-J rotational levels in energy. It is defined as $\tau = K_a - K_c$. The zero-order energies may be expressed as

$$E^0_{v_1 v_2 \cdots v_{3N-6};\, J\tau} = \sum_{i=1}^{3N-6} E_{v_i} + E_{\text{rot}}(J, \tau, A_{\mathbf{v}}, B_{\mathbf{v}}, C_{\mathbf{v}}). \quad (2)$$

Since formaldehyde is a near-prolate rotor and we are not especially interested in its inertial asymmetry, we will occasionally further simplify to symmetric-rotor language.

All of the terms excluded from H^0 appear in H'. We are concerned here only with the terms in H' which destroy the "goodness" of the basis function labels $\mathbf{v}$ and the τ rotational quantum numbers (rather than the rigorously good quantum numbers such as J, M, and the irreducible representation label of the rotation-vibration product function).

The individual mode vibrational quantum numbers are compromised by two mechanisms: Fermi (potential energy coupling) and Coriolis (kinetic energy coupling) perturbations. Fermi interactions are active even in the nonrotating molecule ($J = 0$),[2] whereas Coriolis interactions affect only $J \neq 0$ levels. Fermi interactions occur only between basis functions belonging to the same *vibrational* symmetry and τ value. Until recently, this had been the IVR mechanism considered to be of primary importance. This paper illustrates the importance of the Coriolis mechanism which compromises both the vibrational and K_a quantum numbers[3] in a way that depends explicitly on J and K_a. First-order Coriolis interactions occur between basis functions belonging to the same *rotation-vibration* symmetry (different vibrational symmetry) and with $\Delta K_a = 0$ (rotation about the a axis in a near prolate top, coupling strength proportional to K_a) or $\Delta K_a = \pm 1$ (rotation about an axis perpendicular to the a axis, coupling strength approximately proportional to $J - K_a$).

The term "spectroscopic perturbation" implies small or occasional departures from the expected regular pattern of energy levels and transition intensities which occurs when an accidental near degeneracy between zero-order basis levels causes a normally negligible term in H' to have observable consequences. When the average vibration-rotation level spacing is much larger than the typical off-diagonal matrix element of H', only a small fraction of spectral transitions will appear to be "perturbed." In addition, the vast majority of perturbations will be simple two-level interactions. There is often no difficulty in assigning perturbed levels and describing them as an explicit mixture of zero-order basis states. Perturbation matrix elements, determined directly from perturbed spectra, contain information about molecular geometry and force constants unavailable from unperturbed spectra.

As the density of states increases, perturbations become the rule rather than the exception. Assignment of such spectra becomes increasingly incomplete and speculative. This results from a multistate interaction (Marcus' "multiple avoided crossings"[4]) whereby each eigenstate contains a significant admixture of several basis states.[1] When, e.g., an eigenstate consists of 21% of basis state $|a\rangle$, 18% of $|b\rangle$, and the remaining 61% is divided among many other $|c\rangle$, $|d\rangle$, . . ., $|n\rangle$, assignment of the state as nominally $|a\rangle$ vs $|b\rangle$ is both difficult and devoid of significance. The multidimensional wave functions corresponding to such states would no longer be expected to have regular nodal structure from which simple assignments could be extracted. (Regular nodal structure implies the existence of a *single* $3N - 6$ dimensional coordinate system with respect to which *all* eigenstates in a given energy region may be distinguished by their node count along each of the $3N - 6$ coordinates.) Consequently, the spectra become *intrinsically* unassignable vibrationally. In this paper, we show how a study of the evolution of molecular spectra from regular to perturbed to intrinsically unassignable provides a detailed picture of which terms in H' are most important for IVR, what are the $\mathbf{v}$, J, and K dependencies of the average matrix elements of H', what is the effective density of rotation-vibration states which participate in a particular type of IVR process, and which classes of zero-order basis states are most reluctant to participate in IVR.

The stimulated emission pumping (SEP) technique[5-8] has made it possible to examine the energy level structure of electronic ground state polyatomic molecules at extremely high levels of vibrational excitation. SEP is a sequential two-photon process. A pulse of the first (PUMP) laser excites the molecule into an electronically excited state. A time-delayed pulse from the second (DUMP) laser stimulates emission to a target rotation-vibration level of the electronic ground state, resulting in a decrease in detected side fluorescence intensity. With the PUMP laser frequency fixed, tuning the DUMP laser permits laser-linewidth limited rotation-vibration spectroscopy at high levels of vibrational excitation, especially when the molecular geometries of the excited and ground electronic states differ significantly.

A crucial distinction between SEP and any single resonance technique is that vibration-rotation spectra are freed of rotational congestion, yet the level structure associated with a wide range of J, K values may be separately and systematically sampled. Thus SEP spectra contain at least as much information as the usual rotationally unselected, high resolution absorption or emission spectrum, but the rotational assignment process is vastly simplified. The ability to identify weak features interspersed among stronger ones is significantly enhanced. Selection of a single rovibronic intermediate level means that it is almost trivial to assign the J, K, and $\mathbf{v}$ quantum numbers of the zero-order basis state from which the spectral intensity is derived. In addition, the J-dependent pattern of energy separations and transition intensities is often sufficient for a complete assignment of Franck–Condon or ΔK forbidden transitions.[8] The present obser-

vation of incompletely assignable fine structure at $J \simeq 10$, $K_a \simeq 2$ in the H_2CO SEP spectra represents an approach toward the intrinsic unassignability of eigenstates expected in the limit of stochastic dynamics. This is the first experimental example where the evolution from highly organized to nearly completely disorganized vibrational behavior may be followed in a fully resolved, J-assigned, eigenstate spectrum. For such a small molecule as H_2CO, if completely disorganized vibrational behavior can be defined, this definition must be quite different from "statistical limit" behavior of larger molecules. No Lorentzian broadening of individual rotation-vibration eigenstates of the H_2CO $\tilde{X}\ ^1A_1$ state is expected or observed here; however, the clumping of individual, resolved eigenstates under Lorentzian envelopes is discussed in Refs. 7 and 27.

We report and discuss rotation-vibration spectra from three spectral features between 7400 and 8600 cm^{-1} of the H_2CO $\tilde{X}\ ^1A_1$ state where the total vibrational density of states is $\rho_v \simeq 0.1$ per cm^{-1}. These features are associated with Franck–Condon allowed transitions into three zero-order vibrational levels: (1) a $2_2 4_4$ vibrational level free from Fermi interaction with other vibrational levels at low J, (2) a $2_3 4_2$ level in strong Fermi interaction with a spectroscopically inactive $1_1 2_1 3_2$ level; this Fermi coupling allows two almost equal intensity lines to appear in the $J = 0$ spectrum and the rotation-vibration spectra show the effects of Coriolis perturbations of both vibrational levels by other spectroscopically inactive levels, and (3) a $1_1 2_2 4_2$ level which is also free from Fermi interaction with other levels, as evidenced by its low J purity. The 2_5 level, which also has intrinsic oscillator strength, lies near the $1_1 2_2 4_2$ level. However, we later show that 2_5 is almost free from Coriolis perturbation. Hence the rotation-vibration spectra of the third feature, apart from a single 2_5 line at any J, K_a, K_c, result from the $1_1 2_2 4_2$ level and its J, K_a-dependent Coriolis interactions with spectroscopically inactive levels in the same energy region. The notation for the normal mode vibrations is explained in Table I. The spectral data consist of level spacings and relative intensities vs J and K_a. At low J values, Fermi matrix elements may be derived from the spectral data by standard deperturbation procedures. At higher J, K_a values, average values of Coriolis matrix elements may be inferred from observed intensity and level spacing distributions. These empirical matrix elements are compared to values computed from a normal mode model which neglects the observed intramode anharmonicity (Sec. III).

TABLE I. Normal mode vibrations of $\tilde{X}\ ^1A_1$ formaldehyde.

Mode	Symmetry species	Vibrational motion	Fundamental frequency (cm^{-1})[a]
ν_1	a_1	Symmetric CH stretch	2782.5
ν_2	a_1	CO stretch	1746.0
ν_3	a_1	HCH bend	1500.2
ν_4	b_1	Out-of-plane bend	1167.3
ν_5	b_2	Antisymmetric CH stretch	2843.3
ν_6	b_2	HCO bend	1249.1

[a] From Ref. 11.

II. EXPERIMENTAL

The experimental scheme and apparatus of SEP have been described previously[5,6] and are briefly summarized here. A Nd:YAG laser (Quanta-Ray DCR-1A) was used to excite two dye lasers (Quanta-Ray PDL-1) simultaneously. The output of one dye laser with Carbazine 720 dye was frequency doubled by a KD*P crystal to provide 1 mJ, 6 ns (FWHM), 0.06 cm^{-1} FWHM PUMP pulses near 354 nm. The second dye laser, with Coumarin 480 or 500 dye, produced DUMP pulses of several mJ and 0.04 cm^{-1} FWHM. The DUMP pulse was temporally delayed by 14 ns relative to the PUMP pulse before it entered the gas cell in spatial overlap with the region previously traversed by the PUMP beam. Both PUMP and DUMP beams were spatially filtered and collimated to 2 mm diameter.

In preparing to record an SEP spectrum from a specific $\tilde{A}$-state rotation-vibration level, the PUMP laser was first pressure scanned with N_2 gas to acquire a fluorescence excitation spectrum of a portion of the formaldehyde $\tilde{A}\ ^1A_2$–$\tilde{X}\ ^1A_1$ 4_0^1 band. Once this spectrum was rotationally assigned,[9] the PUMP laser was tuned to and then held fixed at the frequency of a selected rovibronic transition. The DUMP laser was then pressure scanned with SF_6 gas over a 35 cm^{-1} range to record the stimulated emission spectrum for a selected energy region in the $\tilde{X}\ ^1A_1$ state.

The SEP signal was detected by a dual photomultiplier-boxcar assembly (PAR 162/165) as a decrease of the side fluorescence intensity. A $^{130}Te_2$ absorption spectrum (at 700 °C) and the transmission fringes from a calibrated etalon (free spectral range 0.5 cm^{-1}) were recorded simultaneously along with the SEP spectrum to provide absolute and relative calibration for the DUMP laser frequency.

Formaldehyde pressures between 50 and 90 mTorr were used. The formaldehyde gas was prepared by pyrolysis of paraformaldehyde and was fractionally distilled twice before use.

III. RESULTS

Rotation-vibration levels near 7460, 8050, and 8530 cm^{-1} in the $\tilde{X}\ ^1A_1$ state were examined by SEP with the $\tilde{A}\ ^1A_2$, $v_4' = 1$ state as the intermediate level. The spectra for these three regions are shown in Figs. 1–3, respectively.

In all three cases, the predominant rotational branch structures were found to be electric dipole b-type, corresponding to the transition moment lying in the H_2CO molecular plane but perpendicular to the CO axis (a axis). The b-type selection rules are $J' - J = 0, \pm 1$, $K_a' - K_a = \pm 1$, and $K_c' - K_c = \pm 1$ for an asymmetric top. (For clarity the rotational quantum numbers will be indicated as $J''_{K_a'',K_c''}$ for the $\tilde{X}\ ^1A_1$, $v'' = 0$ level, $J'_{K_a',K_c'}$ for the $\tilde{A}\ ^1A_2$, $v_4' = 1$ level, and J_{K_a,K_c} for the high vibrational levels of the $\tilde{X}\ ^1A_1$ state.) The rotational assignments in the figures

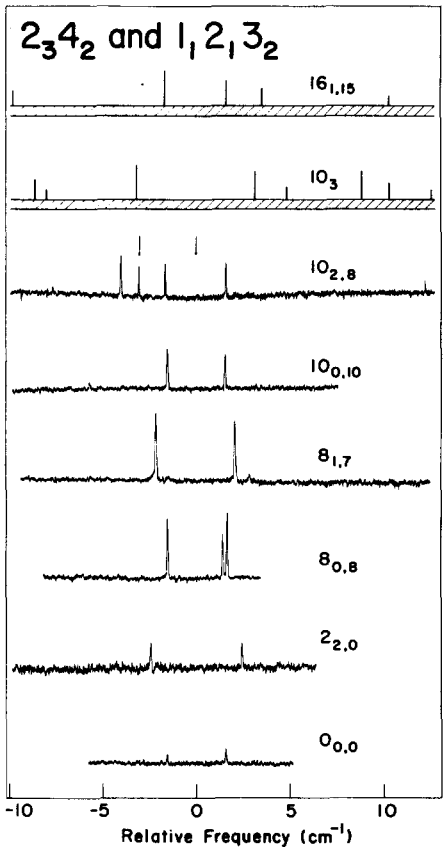

FIG. 1. The SEP $\tilde{A}\ 4^1$–$\tilde{X}$ rotation-vibration spectra near the $2_3 4_2$ and $1_1 2_1 3_2$ levels of the $\tilde{X}$ state. The vibrational term values are 7462 and 7459 cm^{-1}, respectively. All lines in the spectra are associated with the $\tilde{X}$ state J, K_a, K_c value specified above the spectrum. Several spectra are unmodified SEP spectra; others are presented as stick diagrams because it was necessary to remove some lines that appeared in SEP spectra after proving that they were associated with a different J value. The shaded area of the stick diagrams represents the noise level. The arrows on the $10_{2,8}$ spectrum indicate the expected positions of the two rotation-vibration levels calculated using the deperturbed rotational constants from Ref. 10.

indicate J_{K_a,K_c}. *All assignments were confirmed by at least two sets of experiments with different* $J'_{K'_a,K'_c}$ *as intermediate levels.* For example, the $J_{K_a,K_c} = 10_{2,8}$ spectrum was obtained as the ^PQ branch from $J'_{K'_a,K'_c} = 10_{1,9}$ as well as the ^PR branch from $9_{1,9}$. Stick diagrams instead of real spectra are shown for some of the rotational levels in the figures for two reasons: (i) the energy scales (laser frequency scanning rate) were not identical in all experiments; (ii) spurious lines owing to accidental overlap of the PUMP frequency with rotational transitions populating levels other than the desired $J'_{K'_a,K'_c}$ level were deleted since they did not appear in a second spectrum from a different $J'_{K'_a,K'_c}$ level. Only lines with S/N ratio larger than one and confirmed by two different experiments are plotted on Figs. 1–3. The PUMP and DUMP transitions leading to $10_{3,7}$ and $10_{3,8}$ are not resolvable by the laser linewidth limited resolution. Thus the asymmetry doublet is denoted by 10_3.

It was observed that two vibrational lines appear at low rotational quantum numbers ($J \leqslant 3$, $K_a \leqslant 1$) in the SEP spectrum at 7460 cm^{-1}. One is present in the 8050 cm^{-1} spectrum, and two in the 8530 cm^{-1} spectrum.

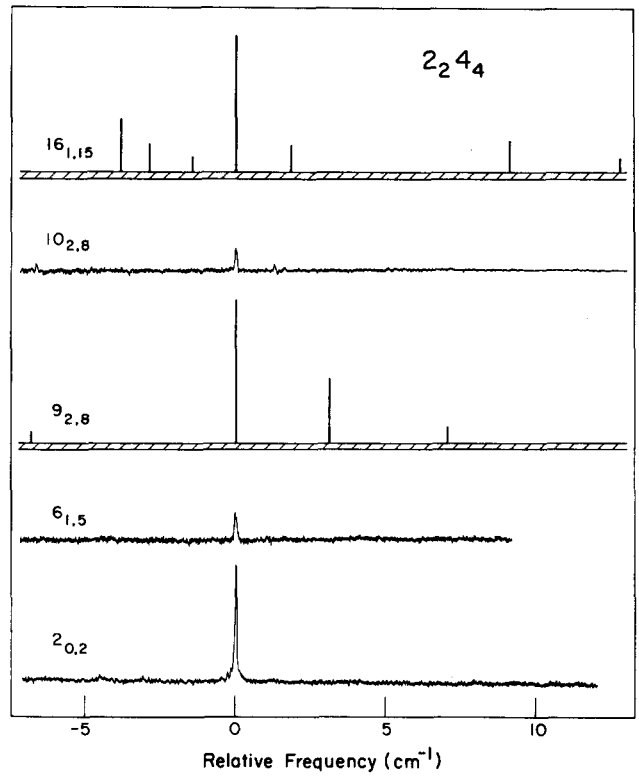

FIG. 2. The SEP $\tilde{A}\ 4^1$–$\tilde{X}$ rotation-vibration spectra near the $\tilde{X}\ ^1A_1$ $2_2 4_4$ level. The vibrational term value is 8044 cm^{-1}.

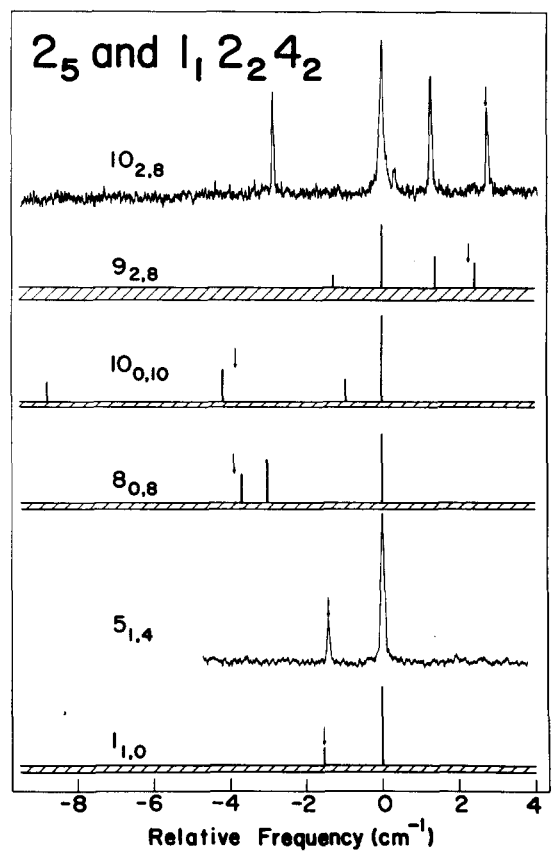

FIG. 3. The SEP $\tilde{A}\ 4^1$–$\tilde{X}$ rotation-vibration spectra near the 2_5 and $1_1 2_2 4_2$ levels. The vibrational term values are 8533 and 8535 cm^{-1}, respectively. The arrows indicate the positions of the 2_5 vibrational levels calculated for the specified rotational quantum numbers using the effective rotational constants deduced from the low J rotational levels.

Definitive vibrational assignments in terms of normal mode quantum numbers can be made for these lines based on the rotational band type, the vibrational term value, the relative intensity, and the effective B and C rotational constants. A detailed account of the assignments of these and a large number of other transitions appears in Ref. 8. The vibrational assignments are shown at the top of the figures.

The transition from $\tilde{A}\ 4^1$ into the $1_12_13_2$ level at 7460 cm^{-1} should have negligible Franck–Condon intensity. It appears at reasonable intensity in the spectrum only by borrowing intensity from the 2_34_2 level through Fermi-type interaction. A detailed deperturbation analysis of this Fermi interaction was performed and will be reported separately.[10] The analysis shows that the rotationless levels of the two deperturbed states are separated by 1.2 cm^{-1} and that the interaction matrix element is 1.5 cm^{-1}.

The transitions from $\tilde{A}\ 4^1$ into the 2_5 and $1_12_24_2$ levels at 8530 cm^{-1} both have appreciable intrinsic Franck–Condon intensities. The energy and intensity patterns for transitions into these two vibrational levels at low rotational quantum numbers give no indication of any significant perturbation interaction between them.

With increasing rotational excitation, the number of lines in the SEP spectra increases. Extra lines begin to appear at $J \gtrsim 8$. Their number increases as either J or K_a increases. For rotational states with $K_a = 0$, no extra lines appeared for $J \leqslant 10$ except in the isolated instance of the $8_{0,8}$ level. When $K_a = 1$ or 2, extra lines were first observed when $J \geqslant 6$. At high J and K_a, the density of lines reaches 0.4 per cm^{-1} for the transitions shown in Fig. 1 and 0.5 per cm^{-1} for those in Figs. 2 and 3. These values are several times larger than the vibrational state densities calculated by direct counting of anharmonic levels (see Sec. IV).

In the spectral region of the transitions into the 2_24_4 vibrational level a strong line can always be found at the center of the cluster of lines, but in the region of the $2_34_2 \sim 1_12_13_2$ Fermi dyad the intensity distribution of the observed lines is more even. In the latter case the unperturbed energies of the 2_34_2 and $1_12_13_2$ vibrational levels are near the center of the group of lines, as indicated for the $10_{2,8}$ level by the vertical arrows in Fig. 1. The $10_{2,8}$ rotational energies of the 2_34_2 and $1_12_13_2$ vibrational levels are calculated from rotational constants and vibrational term values obtained from a deperturbation analysis of the low rotational levels.[10] In the region of the $2_5 - 1_12_24_2$ pair of levels, the effective rotational constants obtained at low J values of the 2_5 level predict rotational energies always near one of the many lines appearing in the spectra of Fig. 3.

IV. DISCUSSION

A. Rotation induced vibrational mixing

In order to confidently attribute the extra spectral lines appearing at high J, K_a rotational quantum numbers exclusively to rotation-induced vibrational mixing in the $\tilde{X}$ state, we must eliminate alternative explanations. These alternatives and the arguments against them are given in the numbered paragraphs below.

(1) Other spectroscopically active vibrational levels could give rise to extra lines at some J_{K_a,K_c} levels but not at others either because the "spurious" vibrational level has rotational constants very different from the level under examination or because the DUMP transitions are of a different rotational branch (e.g., $\Delta J = 1$, $\Delta K_a = 1$ rather than $\Delta J = 0$, $\Delta K_a = -1$). In either of these cases, the difference in separation between consecutive members of the target and spurious rotational branches could cause near coincidence for certain J_{K_a,K_c} values but not others.

Table II shows that there are no vibrational levels expected to have appreciable transition strength from $\tilde{A}\ 4^1$ which lie within ± 80 cm^{-1} of the vibrational levels assigned in Figs. 1–3. Recall that the intensities of the $\tilde{A} \rightarrow \tilde{X}$ vibrational transitions observed here depend upon the Franck–Condon factors between the $\tilde{X}\ ^1A_1$ vibrational levels and $\tilde{A}\ ^1A_2$ $v'_4 = 1$. The choice of normal mode product functions as a zero-order basis for the vibrational wave functions has been shown to be effective in estimating the relative intensities of vibrational bands both in absorption and in fluorescence spectra.[12,13] A complete set of anharmonic vibrational constants ($6\omega_i$ and $21X_{ij}$) was determined for the $\tilde{X}\ ^1A_1$ state.[8] These constants can be used to calculate the energies of vibrational levels for any set of normal mode quantum numbers. The vibrational levels in the three energy regions corresponding to Figs. 1–3 are listed in Table II. It has been established that only the $2_n^04_m^1$ and $1_1^02_n^04_m^1$ b-type transitions from the $\tilde{A}\ 4^1$ level have significant Franck–Condon factors[12–15] (oscillator strength $\gtrsim 10^{-6}$). Transitions of a-type or c-type and other b-type transitions are several orders of magnitude weaker. It is not plausible that either differences in rotational constants or different rotational branches could cause another Franck–Condon allowed level, with a rotationless origin removed by more than 80 cm^{-1}, to appear in the SEP spectra for $J_{K_a,K_c} = 16_{1,15}$ or 10_3.

(2) Rotation-vibration interaction in the $\tilde{A}$ state causes rotationally dependent mixing that modifies selection rules and Franck–Condon factors in the $\tilde{A} \rightarrow \tilde{X}$ transition. Although Lee and co-workers[16] have documented Coriolis perturbations on the 6_6 and 8_8 rotational levels in the 5^1 and 1^14^1 vibrational levels of $\tilde{A}\ ^1A_2$ formaldehyde, there is no plausible candidate for strong Coriolis mixing with 4^1. The $\tilde{A}$ state vibrational level that would couple most strongly to 4^1 is the 6^1 level which couples via an a-axis Coriolis interaction. These two vibrational levels are more than 1000 cm^{-1} apart. Even for $K'_a = 3$ rotational levels, the mixing coefficient arising from a-axis Coriolis interaction would be smaller than a few percent. The vibrationless level, though it is only 125 cm^{-1} from the 4^1 level, cannot couple effectively with 4^1. Coriolis interaction between levels differing by only one vibrational quantum is typically weak (see below, this section).

(3) Satellite lines appear due to collision induced rotational relaxation in the $\tilde{A}$ state. Collisions have a

TABLE II. Anharmonic normal mode vibrational levels near 7460, 8050, and 8530 cm^{-1} calculated from the vibrational constants of Ref. 8.

Calculated vibrational energy (cm^{-1})[a]	Normal mode assignment	Symmetry species	Calculated vibrational energy (cm^{-1})[a]	Normal mode assignment	Symmetry species
7388	$2_1 3_3 6_1$	b_2	8058	$1_1 3_1 4_1 5_1$	a_2
7396	$3_1 4_3 6_2$	b_1	8068	$1_1 3_1 5_1 6_1$	a_1
7400	$1_1 2_2 4_1$	b_1	8075	$5_2 6_2$	a_1
7418	$2_2 3_1 6_2$	a_1	8081	$1_2 3_1 6_1$	b_2
7421	$2_2 4_1 5_1$	a_2	8083	$1_1 2_1 4_1 6_2$	b_1
7421	$4_4 5_1$	b_2	8090	$2_1 4_2 5_1 6_1$	a_1
7426	$1_1 4_3 6_1$	a_2	8107	$1_2 3_1 4_1$	b_1
7448	6_6	a_1	8123	$2_1 3_1 6_4$	a_1
7456	$3_1 4_2 6_3$	b_2	8130	$2_3 3_2$	a_1
7464	$2_3 4_2$[b]	a_1	8470	$3_1 4_5 6_1$	a_2
7468	$1_1 2_1 3_2$	a_1	8479	$2_2 3_1 4_2 6_1$	b_2
7470	$1_1 2_2 6_1$	b_2	8484	$2_1 3_1 5_1 6_2$	b_2
7475	$1_1 2_2 6_2$	a_1	8496	$2_1 4_1 5_2$	b_1
7484	$2_1 4_5$	b_1	8503	$2_2 6_4$	a_1
7499	3_5	a_1	8504	$3_3 5_1 6_1$	a_1
7509	$4_3 5_1 6_1$	b_1	8505	$1_1 4_5$	b_1
7513	$3_1 4_1 6_4$	b_1	8510	$3_3 4_1 5_1$	a_2
7520	$4_7 6_1$	a_2	8514	$4_2 6_5$	b_2
7526	$2_2 5_1 6_1$	a_1	8525	$2_1 3_3 4_2$	a_1
7971	$2_3 5_1$	b_2	8533	2_5[b]	a_1
7972	$3_3 4_2 6_1$	b_2	8537	$1_1 2_2 4_2$[b]	a_1
7973	$3_3 4_1 6_2$	b_1	8537	$3_1 4_4 6_2$	a_1
7986	$2_1 3_1 4_2 6_2$	a_1	8540	$2_1 3_3 4_1 6_1$	a_2
7993	$2_1 6_5$	b_2	8550	$4_5 5_1$	a_2
7994	$2_1 4_3 5_1$	a_2	8551	$2_1 3_3 6_2$	a_1
8002	$4_1 5_2 6_1$	a_2	8554	$2_2 4_2 5_1$	b_2
8004	$2_4 4_1$	b_1	8561	$1_1 4_4 6_1$	b_2
8013	$1_1 3_2 6_2$	a_1	8564	$2_2 3_1 4_1 6_2$	b_1
8024	$1_1 2_1 4_2 6_1$	b_2	8583	$2_1 5_2 6_1$	b_2
8027	$1_1 3_2 4_1 6_1$	a_2	8597	$2_3 4_3$	b_1
8038	$1_1 3_2 4_2$	a_1	8598	$4_1 6_4$	b_1
8039	4_7	b_1	8599	$3_5 6_1$	b_2
8046	$2_2 4_4$[b]	a_1	8601	$3_1 4_3 6_3$	a_2
8047	$1_1 5_2$	a_1	8610	$1_1 2_2 4_1 6_1$	a_2
8056	$2_1 3_1 4_1 6_3$	a_2			

[a] The standard deviation of the calculation is 3.3 cm^{-1}, Ref. 8.

[b] $\tilde{X}$-state vibrational levels with strongest oscillator strength from the $\tilde{A}\ 4^1$ level. Franck–Condon factors for transitions from $\tilde{A}\ ^1A_2\ 4^1$ to other rotationless vibrational levels of $\tilde{X}\ ^1A_1$ are at least three orders of magnitude weaker.

negligible effect on SEP spectra (in marked contrast to dispersed fluorescence spectra). Even at the highest pressure (90 mTorr) used in these SEP experiments, the mean time between inelastic collisions is almost seven times longer than the 14 ns delay between the PUMP and DUMP pulses.[17] No rotational relaxation in the $\tilde{A}$ state is expected or observed during this short delay.

Hence, the appearance of additional lines in SEP spectra at higher J, K_a values must arise from mixing between the normal mode levels of the $\tilde{X}$ state. This leads to the sharing of intensity among the rotation-vibration eigenstates which have acquired an appreciable admixture of the single basis function carrying oscillator strength.

It is useful at this point to review the general rules for Coriolis interactions. The two most important aspects of the Coriolis effect are the symmetry of the vibration-rotation levels and the magnitude of the matrix elements between the interacting zero-order rotation-vibration levels, especially their explicit dependence on the rotational quantum numbers. The symmetry constraint determines the density of vibration-rotation levels that may interact. The magnitude of the matrix elements governs the extent of mixing.

The Coriolis interaction matrix element between two zero-order vibration-rotation levels can be calculated from a normal mode analysis, since the zero-order basis set is chosen to be the products of normal mode functions. The zero-order basis state $|\mathbf{v}, J_{K_a}, K_c\rangle$ is an eigenfunction of the Hamiltonian

$$H^0 = \frac{1}{2}\sum_\alpha \frac{P_\alpha^2}{I_{\alpha\alpha}^0} + \frac{1}{2}\sum_i (p_i^2 + 4\pi^2 c^2 \omega_i^2 q_i^2), \tag{4}$$

where $\mathbf{v}$ represents the set of vibrational quantum numbers which specify the vibrational basis function, P_α the total angular momentum operator about the $\alpha = (a, b, c)$ axis, $I_{\alpha\alpha}^0$ the equilibrium geometry moment of inertia, p_i the linear vibrational momentum of normal coordinate q_i, ω_i the harmonic frequency, and c the speed of light.

The complete rotation-vibration Hamiltonian of polyatomic molecules has been expanded in normal coordinates by Nielson and co-workeres.[18,19] For evaluating matrix elements, rather than computing eigenvalues, the Hamiltonian prior to simplification by contact transformation should be used. The kinetic energy terms in H' that would induce coupling between different normal mode states are listed in Table III according to the

TABLE III. Terms in the Hamiltonian that contribute to rotation-vibration interactions between vibrational levels differing by ΔV quanta.[a]

ΔV	Primary term[b]	Secondary term[b]
2	$-\sum_{\alpha} \frac{\Pi_\alpha P_\alpha}{I^0_{\alpha\alpha}}$	$\frac{1}{2}\sum_{\alpha,\beta,i,j} \frac{\Omega^{(2)\alpha\beta}_{ij}}{I^0_{\alpha\alpha} I^0_{\beta\beta}} q_i q_j P_\alpha P_\beta$
3	$-\sum_{\alpha,\beta,i} \frac{\Omega^{(1)\alpha\beta}_{i}}{I^0_{\alpha\alpha} I^0_{\beta\beta}} q_i \Pi_\alpha P_\beta$	$\frac{1}{2}\sum_{\alpha,\beta,i,j,k} \frac{\Omega^{(3)\alpha\beta}_{ijk}}{I^0_{\alpha\alpha} I^0_{\beta\beta}} q_i q_j q_k P_\alpha P_\beta$
4	$-\sum_{\alpha,\beta,i,j} \frac{\Omega^{(2)\alpha\beta}_{ij}}{I^0_{\alpha\alpha} I^0_{\beta\beta}} q_i q_j \Pi_\alpha P_\beta$	$\frac{1}{2}\sum_{\alpha,\beta,i,j,k,l} \frac{\Omega^{(4)\alpha\beta}_{ijkl}}{I^0_{\alpha\alpha} I^0_{\beta\beta}} q_i q_j q_k q_l P_\alpha P_\beta$
5	$-\sum_{\alpha,\beta,i,j,k} \frac{\Omega^{(3)\alpha\beta}_{ijk}}{I^0_{\alpha\alpha} I^0_{\beta\beta}} q_i q_j q_k \Pi_\alpha P_\beta$	$\frac{1}{2}\sum_{\alpha,\beta,i,j,k,l,m} \frac{\Omega^{(5)\alpha\beta}_{ijklm}}{I^0_{\alpha\alpha} I^0_{\beta\beta}} q_i q_j q_k q_l q_m P_\alpha P_\beta$
	$\Omega^{(1)\alpha\beta}_i = -a^{\alpha\beta}_i, \quad \Omega^{(2)\alpha\beta}_{ij} = \frac{3}{4}\sum_{\gamma} \frac{a^{\alpha\gamma}_i a^{\gamma\beta}_j}{I^0_{\gamma\gamma}}$	
	$\Omega^{(3)\alpha\beta}_{ijk} = -\frac{1}{2}\sum_{\gamma\delta} \frac{a^{\alpha\gamma}_i a^{\gamma\delta}_j a^{\delta\beta}_k}{I^0_{\gamma\gamma} I^0_{\delta\delta}}, \quad \Omega^{(4)\alpha\beta}_{ijkl} = \frac{5}{16}\sum_{\gamma\delta\xi} \frac{a^{\alpha\gamma}_i a^{\gamma\delta}_j a^{\delta\xi}_k a^{\xi\beta}_l}{I^0_{\gamma\gamma} I^0_{\delta\delta} I^0_{\xi\xi}}$	
	$\Omega^{(5)\alpha\beta}_{ijklm} = -\frac{3}{16}\sum_{\gamma\delta\xi\theta} \frac{a^{\alpha\gamma}_i a^{\gamma\delta}_j a^{\delta\xi}_k a^{\xi\theta}_l a^{\theta\beta}_m}{I^0_{\gamma\gamma} I^0_{\delta\delta} I^0_{\xi\xi} I^0_{\theta\theta}}$	

[a] All notation in this table is defined in Sec. IV.
[b] The primary terms depend linearly on P_α while the secondary terms depend on $P_\alpha P_\beta$.

difference in normal mode quantum numbers of the coupled states $\Delta V = \sum_i |\Delta v_i|$. In Table III, Π_α, the vibrational angular momentum, is defined as

$$\Pi_\alpha = \sum_{ij} \zeta^\alpha_{ij} q_i p_j,$$

in which the coefficients ζ^α_{ij} are the Coriolis coupling constants. The terms linear in P_α are called primary. Secondary terms are proportional to $P_\alpha P_\beta$. The primary term does not exist for $\Delta V = 1$. Secondary terms for $\Delta V = 1$ are also left out of Table III because two vibrational levels that differ by only one vibrational quantum must be separated by at least 1000 cm^{-1} in the $\tilde{X}\ ^1A_1$ state of formaldehyde. Coriolis interaction for the J, K_a values of interest here between such widely spaced levels would be negligible.

The Coriolis matrix element can be separated into a vibrational and a rotational part. The rotational part contains only the P_α's. The $\langle J_{K_a,K_c}|P_\alpha|J'_{K'_a,K'_c}\rangle$, $\langle J_{K_a,K_c}|P_\alpha P_\beta|J'_{K'_a,K'_c}\rangle$ matrix elements are summarized in Table IV. Formaldehyde is a near-prolate asymmetric top ($\kappa = -0.9610$ for $v = 0$), thus the rotational wave functions can be approximated by symmetric top wave functions $|J_K\rangle$ as $|J_{K_a,K_c}\rangle \cong 2^{-1/2}(|J_K\rangle \pm |J_{-K}\rangle)$ for $K_a = K > 0$, and $|J_{0,J}\rangle \cong |J_0\rangle$.[20] It is apparent from Table IV that the a-axis Coriolis matrix elements are proportional to K_a whereas the b- and c-axis matrix elements are approximately proportional to $J - K_a$. This explicit rotational quantum number dependence, combined with SEP's unique ability to select a specific rotation-vibration level, allows us to "switch on or off" a particular Coriolis interaction mechanism and to examine systematically its effect on vibrational mixing.

Table IV shows that the Coriolis interaction conserves only the total angular momentum, but not its projection onto any molecular axis. The selection rules for a-axis Coriolis interactions are $\Delta K_a = 0$, $\Delta K_c = \pm 1$. For b-axis interactions they are $\Delta K_a = \mp 1$, $\Delta K_c = \pm 1$, and for c-axis interactions they are $\Delta K_a = \pm 1$, $\Delta K_c = 0$. Hence b- and c-axis Coriolis interactions could allow interaction between different K_a components of two vibrational levels separated by $\sim|K_a^2 - (K_a \pm 1)^2|[A - (B + C)/2]$ at their rotationless origins. Coriolis interactions through higher order rotational terms in the Hamiltonian, e.g., the secondary terms in Table III containing $P_\alpha P_\beta$, further relax the ± 1 selection rules for ΔK_a and ΔK_c. Even with only the primary terms, it is clear from Fig. 4(a) that all same-J rotational levels can interact with each other through Coriolis mechanisms. Thus Coriolis interactions tend to destroy the goodness of the K_a, K_c quantum numbers.[3]

TABLE IV. Matrix elements of the total angular momentum P_α for a near-prolate top.[a]

$$\langle J_{K_a,K_c}|P_a|J_{K_a,K_c\pm 1}\rangle \approx \hbar K_a$$

$$\langle J_{K_a,K_c}|P_b|J_{K_a\mp 1,K_c\pm 1}\rangle \approx \pm\frac{i\hbar}{2}[J(J+1) - K_a(K_a \mp 1)]^{1/2}\ ^b$$

$$\langle J_{K_a,K_c}|P_c|J_{K_a\pm 1,K_c}\rangle \approx \frac{\hbar}{2}[J(J+1) - K_a(K_a \pm 1)]^{1/2}$$

$$\text{for } K_a = 0, \quad \langle J_{0,J}|P_b|J_{1,J-1}\rangle \approx -i\hbar 2^{-1/2}[J(J+1)]^{1/2\ b}$$

$$\langle J_{0,J}|P_c|J_{1,J}\rangle \approx \hbar 2^{-1/2}[J(J+1)]^{1/2}$$

$$\langle J_{K_a,K_c}|P_\alpha P_\beta|J_{K'_a,K'_c}\rangle = \sum_{K''_a,K''_c} \langle J_{K_a,K_c}|P_\alpha|J_{K''_a,K''_c}\rangle\langle J_{K''_a,K''_c}|P_\beta|J_{K'_a,K'_c}\rangle$$

[a] The $\approx$ sign comes from the approximate expansion of the near-prolate rotational wave functions in terms of the prolate top functions.
[b] This phase choice implies identification of the a (C–O bond), b (in plane), and c (perpendicular to plane) inertial axes with z, y, and x, respectively.

The equilibrium configuration of the $\tilde{X}\ ^1A_1$ state of formaldehyde has C_{2v} symmetry. The rotational wave functions can be classified into the four irreducible representations of C_{2v} according to the evenness and oddness of the K_a and K_c quantum numbers.[21] The breakdown of the K-quantum numbers corresponds to mixing of rotational levels belonging to different symmetry species. The vibrational symmetry in Coriolis interactions was first discussed by Jahn.[22] In the $\tilde{X}\ ^1A_1$ state of formaldehyde, a vibrational level belonging to any of the four irreducible representations can interact with levels of each of the other three representations through rotation about the a, b or c axes, as indicated in Fig. 4(b). Each zero-order vibrational level can interact with any other level via either Fermi or Coriolis perturbation terms. Thus vibrational symmetry as well as the zero-order vibrational quantum number is destroyed by Coriolis interactions. The vibration-rotation interaction preserves only the *total vibration-rotation symmetry.*

The K_a, K_c pseudodegeneracy for each value of J is $2J + 1$. The total rotation-vibration level density for a specific J value is then $(2J + 1)\rho_v$, ρ_v being the density of vibrational levels. Among all these levels, the ones that would participate in the sharing of oscillator strength of the spectroscopically active zero-order vibration-rotation level of a specified vibration-rotation symmetry would have a density of $\sum_\Gamma \rho_\Gamma N_\Gamma$, where ρ_Γ is the density of vibrational levels of the Γ symmetry species, and N_Γ is the number among the $(2J + 1)$ rotational multiplicity that have the correct vibration-rotation symmetry. This quantity can be well approximated by $(2J + 1)\rho_v/4$ for the $\tilde{X}$ state of formaldehyde; the factor $1/4$ reflects the four symmetry species in the C_{2v} group.[23,24]

All of our experimental observations can be understood from the above features of Coriolis interactions. The general trend of increasing numbers of observed spectral lines as J and K_a increase results from both the increase in the matrix elements with K_a or $J - K_a$ and the increasing density of vibration-rotation levels among which spectral intensity is shared. The fact that the observed spectral line densities are larger than the calculated *vibrational* level density is a strong indication that Coriolis mechanisms are at work. ρ_v can be calculated from Table II to be 0.13 per cm^{-1} at 7460 cm^{-1}, 0.16 at 8050 cm^{-1}, and 0.15 at 8530 cm^{-1}. This is about three times smaller than the observed densities of lines in Figs. 1–3. The factor of 3 is smaller than $(2J + 1)/4$ for $J = 10$ and 16. Nonetheless, it indicates substantial τ mixing.[3]

There are some subtleties in the experimental data that should be noted. The spectra show that the a-axis Coriolis interaction alone is not sufficient to cause a noticeable intensity sharing among low J levels with $K_a = 1$ (see Figs. 1–3). This is true also for the case of the $2_{2,0}$ level (Fig. 1). The same comparison can be made for b- and c-axis Coriolis interactions. Up to $J = 10$, little intensity sharing was observed for $K_a = 0$ except at the $8_{0,8}$ level in Fig. 1, where an accidental degeneracy occurs. This suggests that the density of vibrational levels with A_2 (or B_1 and B_2) symmetry in the vicinity of the

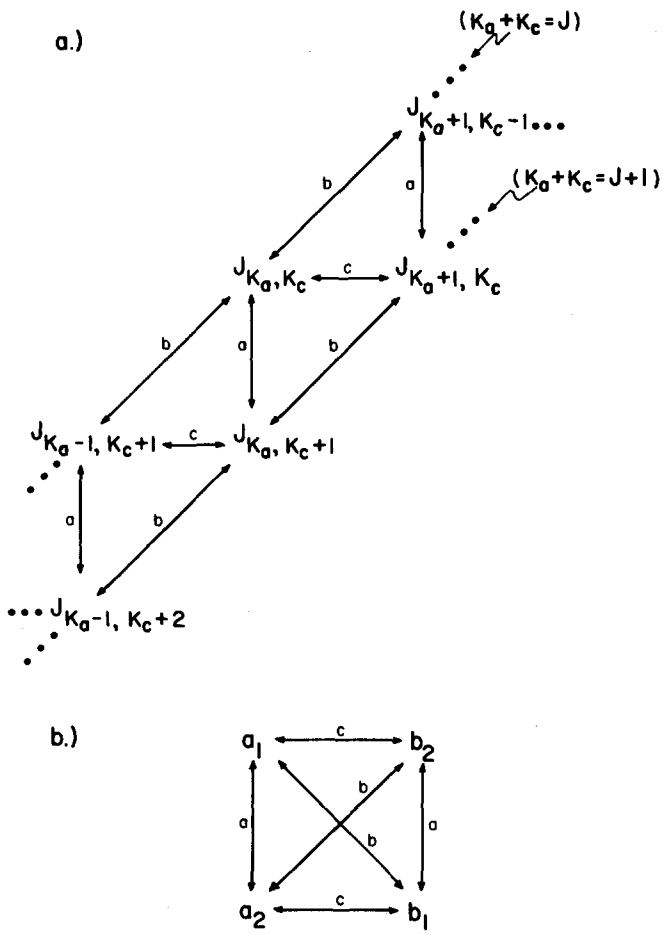

FIG. 4. Coriolis coupling diagrams for a C_{2v} symmetry molecule: (a) coupling among rotational levels; (b) coupling among the four types of vibrational symmetry levels. The letter above the arrow-line indicates the axis of rotation by which the two levels are coupled.

spectroscopically active level is insufficient to allow the a-axis (or b- and c-axis) Coriolis matrix elements to cause significant mixing. However, it is apparent from the spectra of $J \geq 10$, $K_a \geq 1$ that once Coriolis interactions involving all three rotational axes have been turned on, the combined effects allow extensive vibrational mixing.

B. Calculation of matrix elements and zero-order basis states

The spectra at higher rotational levels in Figs. 1–3 exhibit interactions among many vibration-rotation levels. In contrast to the case of typical spectroscopic perturbations involving only two levels, deperturbation of a many-level system is a formidable and nontrivial task. A full deperturbation analysis for the purpose of determining matrix elements, molecular constants, and assigning the interacting levels would require keeping track of all lines in a series of J_{K_a,K_c} spectra. Without *a priori* knowledge of the precise rotationless origins and rotational constants, the reliability of such a deperturbation would be doubtful, even if it were feasible.

Here, rather than a complete deperturbation analysis, we seek a semiquantitative understanding of the spectra. We calculate the Coriolis matrix elements for a chosen set of zero-order basis states. These calculated matrix

elements combined with the calculated density of vibration-rotation levels provide model spectra. In addition to examination of the rotation-vibration interaction mechanism, the calculated matrix elements allow us to evaluate the adequacy of the chosen zero-order basis states for representing the real eigenstates.

The Coriolis interaction matrix elements were calculated from the results of a standard normal mode analysis. The normal mode analysis is summarized in the Appendix. Table V gives the matrix elements between some harmonic normal mode levels which lie within ±60 cm^{-1} of the spectroscopically active levels in the three energy regions of Figs. 1–3. The 60 cm^{-1} range was chosen because it represents the largest rotationless origin separation between two vibrational levels that could interact strongly through *b*- or *c*-axis Coriolis couplings for the highest K_a investigated (K_a = 3). However, the effects of other levels removed by as much as 120 cm^{-1} (but with large *a*-axis Coriolis matrix elements) should also be considered. These *a*-axis coupled states are also included in Table V.

In the regions of the fundamentals 3_1, 4_1, and 6_1, the effect of Coriolis interaction is to produce only energy shifts in rotational levels. Analyses of spectra in these regions using a prolate top model gave $|\langle 4_1|H'|6_1\rangle| = 10.07(K_a)$ cm^{-1}, $|\langle 4_1|H'|3_1\rangle| = 0.6442f(J, K_a)$ cm^{-1}, and $|\langle 6_1|H'|3_1\rangle| = 0.3768f(J, K_a)$ cm^{-1},[25] where $f(J, K_a)$ is defined in Table V. The Coriolis constants (Table VI) obtained from our normal mode analysis, combined with the rotational constants $A_e = \hbar^2/2I^0_{aa} = 9.580$ cm^{-1}, $B_e = \hbar^2/2I^0_{bb} = 1.303$ cm^{-1}, and $C_e = \hbar^2/2I^0_{cc} = 1.146$ cm^{-1}, derived from the equilibrium structure,[26] allow us to calculate the same matrix elements. These calculated values are 10.3 K_a, $0.76f(J, K_a)$, and $0.33f(J, K_a)$ cm^{-1}, respectively. This leads us to believe that other Coriolis *coupling constants,* for which no experimental checks exist, can be calculated to comparable accuracy, i.e., better than 20%. Hence, Coriolis matrix elements *in the harmonic normal mode basis* would be obtained at the same level of accuracy.

Table V shows that the harmonic basis set calculation does predict additional Coriolis mixed levels to appear in the SEP spectra at higher rotational quantum numbers, though it fails to generate enough levels with sufficiently large matrix elements to correspond to the observed intensity distribution shown in Figs. 1–3. There is a marked discrepancy in the region of the 2_24_4 level. The only plausible extra line would be from the $1_12_14_3$ level. The Coriolis calculation cannot account for the three extra lines observed at $10_{2,8}$ or the five extra lines at $16_{1,15}$. A similar discrepancy exists for the region of the 2_5 and $1_12_24_2$ levels. Two of the three extra lines probably

TABLE V. Coriolis interaction matrix elements calculated in the harmonic normal mode basis.[a]

$\langle v\|$	$\|v'\rangle$	ΔV	Vibrational energy separation (cm^{-1})	$\langle v, J_{K_a,K_c}\|H'\|v', J_{K'_a,K'_c}\rangle$[h]
2_34_2	$1_12_24_1$	3	64	$\mp 0.072f(J, K_a)$
	$2_24_15_1$	3	43	$1.8K_a$
	$2_34_16_1$[b]	2	−126	$14K_a$
$1_12_13_2$	$2_13_34_1$[c]	3	91	$\mp 0.050f(J, K_a)$
	$2_13_36_1$	3	80	$0.050f(J, K_a)$
$1_12_24_1$	$2_24_15_1$	2	−21	$-0.050f(J, K_a)$
	$1_12_26_1$	2	−70	$10.3K_a$
$2_24_15_1$	$1_12_26_1$	4	−49	$\mp 0.0032f(J, K_a)$
$1_12_26_1$	$2_34_16_1$[b]	3	−121	$\mp 0.054f(J, K_a)$
2_14_5	4_45_1	3	62	$-1.6K_a$
2_24_4	$1_12_14_3$[d]	3	85	$\mp 0.083f(J, K_a)$
	$2_14_35_1$	3	53	$-2.1K_a$
	$2_24_36_1$[e]	2	−120	$20K_a$
$2_24_36_1$[e]	$2_14_25_16_1$	3	−46[f]	$1.8K_a$
	$1_12_14_3$[d]	3	85[f]	$0.065f(J, K_a)$
	$1_12_14_26_1$	3	23[f]	$\mp 0.072f(J, K_a)$
$1_12_24_2$	$2_23_14_26_1$	3	58	$0.029f(J, K_a)$
	2_34_3	3	−61	$\pm 0.090f(J, K_a)$
	$1_12_24_16_1$	2	−73	$14K_a$
$1_12_24_16_1$	$2_24_25_1$	4	−18[g]	$\mp 0.0045f(J, K_a)$
	$2_23_14_16_2$	3	−27[g]	$0.041f(J, K_a)$
$3_14_46_2$	$3_14_56_1$	2	67	$-33K_a$
	$1_14_46_1$	3	−24	$+0.022f(J, K_a)$
	$3_14_36_3$	2	−63	$36K_a$

[a] $f(J, K_a) = [J(J+1) - K_a(K_a \pm 1)]^{1/2}$ for $K'_a = K_a \pm 1$.
[b] The calculated vibrational energy is 7591 cm^{-1}.
[c] The calculated vibrational energy is 7377 cm^{-1}.
[d] The calculated vibrational energy is 7961 cm^{-1}.
[e] The calculated vibrational energy is 8166 cm^{-1}.
[f] The difference of vibrational energy is between $|v'\rangle$ and 2_24_4.
[g] The difference of vibrational energy is between $|v'\rangle$ and $1_12_24_2$.
[h] The imaginary matrix elements are made real by multiplying the vibrational wave functions of a_1 and b_1 symmetry by a phase factor $e^{\pm i\pi/2}$.

TABLE VI. Coriolis coupling constants and $a_i^{\alpha\beta}$ coefficients from the normal mode analysis in the Appendix.

Coriolis constants

$\zeta^a_{45} = -0.8428$	$\zeta^b_{14} = -0.5295$	$\zeta^c_{15} = -0.0440$
$\zeta^a_{46} = 0.5381$	$\zeta^b_{24} = 0.6143$	$\zeta^c_{16} = 0.9151$
	$\zeta^b_{34} = 0.5849$	$\zeta^c_{25} = 0.5243$
		$\zeta^c_{26} = -0.3203$
		$\zeta^c_{35} = 0.8503$
		$\zeta^c_{36} = 0.2448$

$a_i^{\alpha\beta}$ coefficients (amu$^{1/2}$ Å)

$(a_i^{aa}) = (2.229, 0.7549, 1.225, 0, 0, 0)$

$(a_i^{bb}) = (0.8431, 5.297, -4.798, 0, 0, 0)$

$(a_i^{cc}) = (3.072, 6.052, -3.573, 0, 0, 0)$

$(a_i^{ab}) = (a_i^{ba}) = (0, 0, 0, 0, -1.339, -2.098)$

$(a_i^{ac}) = (a_i^{ca}) = (a_i^{bc}) = (a_i^{cb}) = (0, 0, 0, 0, 0, 0)$

correspond to the $2_2 3_1 4_2 6_1$ and $2_3 4_3$ levels as a result of coupling to the $1_1 2_2 4_2$ level. In the region of $2_3 4_2 - 1_1 2_1 3_2$, the calculated matrix elements fail to indicate any states capable of significant coupling to the $K_a = 0$ or 1 levels except for $2_3 4_1 6_1$, which, however, lies too far away to appear in the spectra. Nevertheless, a total of five lines appear in the $16_{1,15}$ spectrum within a 20 cm^{-1} range. For the $K_a = 2$ or 3 levels, a-axis Coriolis coupling brings the $2_2 4_1 5_1$ level into range for significant coupling with $2_3 4_2 - 1_1 2_1 3_2$, and b- or c-axis interactions would additionally include $1_1 2_2 4_1$, $1_1 2_2 6_1$, and perhaps $2_1 3_3 6_1$. Nonetheless, the calculated Coriolis matrix elements are too small to account for the intensity distribution in the 10_3 spectrum.

In all the above cases, additional levels will have significant matrix elements with the spectroscopically active level. However, their rotationless origins are too distant for a strong interaction with the spectroscopically active level according to our crude model. A detailed picture for each of the three regions would require knowledge of the rotationless origins and the rotational constants for all vibrational levels. Instead of attempting this, we proceeded in a rough model which incorporated general features such as the local density of levels of each vibrational symmetry and the approximate *average* matrix elements among them.

A spectrum corresponding to a $10_{2,8}$ level of a spectroscopically active A_1 vibrational level between 7000 and 9000 cm^{-1} was computed. The vibrational densities of states for each of the four symmetry species of C_{2v} are $\rho_{a_1} = 0.044$, $\rho_{a_2} = 0.023$, $\rho_{b_1} = 0.028$, and $\rho_{b_2} = 0.036$ per cm^{-1}. Within a 90 cm^{-1} range centered around the active level, there are three additional A_1 levels ($10_{2,8}$), two A_2 levels ($10_{2,9}$), five B_1 levels ($10_{3,7}$ and $10_{1,9}$), and seven B_2 levels ($10_{3,8}$ and $10_{1,10}$). The Fermi matrix elements between the A_1 vibrational levels were assumed to be 2 cm^{-1}. The Coriolis matrix elements for the a-, b-, and c-axis interactions were set at average values of 4, 0.5, and 0.5 cm^{-1} for these rotational quantum numbers according to Table V, as calculated for the $2_3 4_2$, $1_1 2_2 4_2$, and $2_2 4_4$ levels. Diagonalization of a matrix containing nine levels evenly spaced within a 45 cm^{-1} range shows that on the average there should be about two extra lines with intensity > 1% of the total intensity. The number of extra lines varies from 0 to 4 in individual simulations, depending on the energy arrangement of the basis levels. Thus, the model computation does generate some extra lines in the spectrum, but it does not reproduce the details of actual intensity distributions as experimentally observed.

Despite the inadequacy of the harmonic normal mode calculation, there are some notable qualitative successes. One significant result is its failure to predict any level likely to couple strongly to 2_5. This is borne out by the SEP spectrum. Of the many lines in the region of $2_5 - 1_1 2_2 4_2$, there is consistently a single line in each of the higher rotational level spectra (see Fig. 3) that can be assigned to the 2_5 level according to the rotational constants obtained from the lower rotational levels. It seems from the present experimental observations and calculation that the ν_2 overtones retain their vibrational purity much better than the combination levels even for high values of the rotational quantum numbers.

Another informative trend in the model spectrum calculation is found in the behavior of different K_a levels. Recall that the a-axis Coriolis matrix elements are zero for $K_a = 0$ and the ones for b- and c-axis interaction vanish for $K_a = J$. A model calculation for the $10_{0,10}$ level set the a-axis Coriolis matrix elements to zero. The remaining b- and c-axis matrix elements are so small in comparison with the energy level spacings that no intensity borrowing is discernible in the computed spectrum. For the $2_{2,0}$ level, the a-axis matrix elements are large. Since there are only three symmetry allowed rotation-vibration levels within the 45 cm^{-1} interval, however, no extra lines are generated by Coriolis interaction in this simple model computation. These results from the model calculation are in qualitative agreement with the spectra shown in Fig. 1.

There are several possibilities to account for the inadequacy of the harmonic oscillator normal mode calculation for the Coriolis matrix elements. The most prominent of these are discussed below:

1. *Strong first-order a-axis Coriolis effects*

Distant vibrational levels that have large a-axis Coriolis matrix elements with the spectroscopically active states may affect the 20 cm^{-1} region of the SEP spectra shown in Figs. 1–3. Some of these predicted matrix elements are as large as 40 cm^{-1} for $K_a = 2$. These a-axis Coriolis interactions should be prediagonalized (contact transformation) before considering the interactions among the levels within the 20 cm^{-1} interval. The prediagonalized mixed level would still consist predominantly of the spectroscopically active basis state, but its admixed character borrowed from the distant a-axis Coriolis coupled level could allow it to mix with many more nearby basis states. One numerical example is given for the region of 7460 cm^{-1}. The $1_1 2_2 6_1$ level does not interact directly

with the nearby 2_34_2 level, but it could interact indirectly via its small matrix element with the 120 cm^{-1} distant $2_34_16_1$ level which has a large a-axis Coriolis matrix element with 2_34_2. Diagonalization of the mutual interaction between the three rotation-vibration basis levels $2_34_2(10_{2,8})$, $1_12_26_1(10_{1,9})$, and $2_34_16_1(10_{2,9})$ shows that the eigenstate with predominant $1_12_26_1$ character borrows about 1%–10% of its intensity from 2_34_2. In the regions of 2_24_4 and $1_12_24_2$, the a-axis coupled states $2_24_36_1$ and $1_12_24_16_1$ may have the same effect on intensity sharing.

2. Anharmonic effects

It should be noted that the vibrational energies in Table II are calculated using nonzero X_{ij} anharmonicity constants. The wave functions associated with these calculated anharmonic energy levels should be eigenfunctions of a Hamiltonian which contains cubic and quartic anharmonic coupling terms in H', rather than the harmonic oscillator wave functions used in the above Coriolis model. In order to isolate the effect of rotation induced vibrational mixing, the anharmonic interactions among the harmonic basis states should be prediagonalized to provide a set of rotationless vibrational eigenstates which are linear combinations of the harmonic basis states.[2] Since a majority of neighboring normal mode levels differ by more than four vibrational quanta, a treatment of the anharmonic coupling would require detailed knowledge of the cubic and quartic terms in the potential energy function.

It was reported in Sec. III that the pair of levels $1_12_13_2$ and 2_34_2, corresponding to a difference of seven quanta, has a Fermi matrix element of 1.5 cm^{-1}. The possibility of even larger Fermi coupling matrix elements for smaller ΔV cannot be excluded. With $\rho_v \sim 0.1$ per cm^{-1} in the 7000–9000 cm^{-1} region, these anharmonic matrix elements will cause significant coupling among many of the harmonic basis states.

Consider the $3_14_16_2$ level which lies near $1_12_24_2$. $3_14_16_2$ is strongly coupled to three other levels through Coriolis interactions (Table V). The anharmonic coupling between $3_14_16_2$ and $1_12_24_2$ may cause intensity sharing among more levels than are directly Coriolis coupled to $1_12_24_2$.

Using Morse Oscillator basis functions for the three totally symmetric normal mode vibrations ν_1, ν_2, and ν_3, the effect of the diagonal anharmonicities on the Coriolis matrix elements of these modes was examined. The harmonic frequencies and anharmonic constants were taken from Ref. 8. Two calculations were performed. The $1_12_24_2 \sim 1_14_36_2$ b-axis Coriolis matrix element increased threefold from $1.1 \times 10^{-4} f(J, K_a)$ cm^{-1} in the harmonic basis to 2.9×10^{-4} (J, K_a) cm^{-1} in the Morse basis. For $2_34_2 \sim 2_24_15_1$, the value increased only slightly from -1.78 to -1.82 K_a cm^{-1}. It is reasonable to expect that when both the diagonal and off-diagonal anharmonicities are included for all vibrational modes, many interactions corresponding to negligible matrix elements in the harmonic calculation would become significant.

3. Higher order Coriolis effects

The second-order terms in Table III contribute about one order of magnitude less to the matrix element than the first-order terms at $J \sim 10$, $K_a \sim 1$. However, these terms become increasingly important for larger J and K_a values. Since these and other higher order terms relax the ΔK_a, $\Delta K_c = 0$ or ± 1 selection rules and cause mixing between levels with $|\Delta K_a|$, $|\Delta K_c|$ larger than one, they would contribute to the vibrational mixing and intensity sharing in the spectrum by introducing nonzero matrix elements between more vibration-rotation levels.

V. CONCLUDING REMARKS. DYNAMICAL AND SPECTROSCOPIC IMPLICATIONS

The intensity distribution of lines in the SEP spectrum observed from a single $\tilde{A}$-state vibration rotation level provides, in its dependence on rotational quantum numbers of the intermediate level, a clear manifestation of rotation induced vibrational mixing. The principles governing vibration-rotation interaction have been well known for decades. Nonetheless, the extent of Coriolis mixing at moderate rotational excitation and vibrational state density is impressive and unexpected. The present observations substantiate previous conjectures regarding the importance of rotation in molecular dynamics, and they should prompt serious consideration of the rotational effects in many dynamical and spectroscopic problems.

A. Stochasticity

Rotation has often been neglected in discussions of intramolecular vibrational dynamics. At low densities of vibrational levels, rotation should not significantly affect the quasiperiodic behavior typically found in semiclassical calculations. In such regions, Coriolis interactions usually result in small energy shifts of the spectroscopic eigenstates from the values predicted by molecular constants, but the separation between rotational and vibrational motions remains essentially valid except for accidental degeneracies. As the vibrational density of states increases, rotation may accelerate the tendency towards stochastic behavior. Future dynamic models should include nonzero values of J and should treat the interaction between rotation and vibration.

In a separate report,[27] a criterion for chaos in quantum spectra developed by Heller *et al.*[28] has been applied to the vibration-rotation spectra of Figs. 1–3. This work showed that increasing complexity in the spectrum appearing with increasing angular momentum corresponds to *decreasingly* chaotic behavior. This can be understood in terms of an available phase space volume that expands more rapidly as J increases than does the occupied phase space volume.

B. Mode selective excitation

Similar rotational effects are to be expected regardless of whether one chooses a normal or local mode zero-order basis set. For a local mode stretching motion, rotation about an axis perpendicular to the vibrational

linear momentum would result in Coriolis forces on the atoms involved in the stretching motion,[22] thus leading to an intermixing of stretching and bending motions (Fig. 5). These considerations must be borne in mind in attempts to take photochemical advantage of mode selective excitation by lasers. For example, in the cw dye laser excitation of a thermal population of organic molecules at a CH stretching overtone,[29-31] bending and other classes of vibrations will certainly be simultaneously excited owing to Coriolis-mixing effects. A more mode-specific excitation could be achieved for nonrotating molecules, although anharmonic (Fermi) interactions in the isolated molecule and collision-induced rotational thermalization might still be problematic.

Rotation may be used to regulate the vibrational motion of the eigenstates excited by a narrow band laser. The vibrational symmetry restriction of the three classes of Coriolis interactions serves as a control mechanism. This can be used by properly selecting the laser-populated J and K values and by taking advantage of suitable accidental degeneracies between vibrational basis states of desired structural characteristics.

C. Overtone spectroscopy

Hydrogen stretching overtones in the electronic ground state of rotationally thermalized molecules (e.g., benzene) have been shown by intracavity dye laser optoacoustic spectroscopy to distribute their oscillator strength in a near Lorentzian "line" shape.[32] The variation of the linewidths vs vibrational energy has been explained by anharmonic coupling models. It was shown to depend upon the matrix elements of the overtone basis states with other, often identifiable classes of basis states.[33,34] If rotational coupling mechanisms had been included, the intermode matrix elements would have been found to depend strongly upon rotational quantum numbers. Thus it is reasonable to expect that the width of a J-selected overtone band would vary with J. This complicates the analysis of the spectral linewidth of data in which J is not selected. In general, conventional analysis of vibration-rotation spectra at low vibrational energy (or state density) deals explicitly with systematic energy level shifts and intensity variations caused by Coriolis interactions. In regions of higher vibrational density of states one should expect a progressive breakdown of vibrational and K quantum numbers as J increases. This would lead to a strongly J-dependent spectral envelope width and spectral line density.

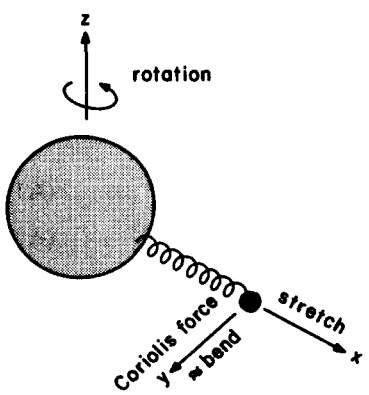

FIG. 5. The filled circle represents one atom in a local mode stretching motion relative to the rest of the molecule (shaded block). Rotation about the z axis causes a Coriolis force on this atom and induces a bending motion, thus mixing the local mode stretching and bending vibrations.

D. Infrared multiphoton excitation

The J and K linewidth dependence may also affect infrared multiphoton excitation mechanisms. In order to explain multiphoton excitation phenomena, the vibrational manifold below dissociation is typically divided into two regions.[35,36] In the lower, discrete region the mismatches between laser frequency and successive absorption transitions due to anharmonic shifts are overcome by power broadening, by rotational compensation, and by degeneracy splitting, etc. In the quasicontinuum, the spectroscopically active basis states spread their oscillator strength over a wide effective linewidth through coupling to a dense manifold of nearby states. This enables the molecule to remain in resonance with the laser frequency throughout the many step absorption to the dissociation continuum. The quasicontinuum must satisfy the criterion[37,38]

$$\Delta\omega_{\text{mol}} \gg \omega_R \gg \rho^{-1}, \tag{5}$$

where $\Delta\omega_{\text{mol}}$ is the effective linewidth, ω_R is the Rabi oscillation frequency, and ρ is the level density. For a given laser intensity, Coriolis mixing at high J values makes it much easier to satisfy both Eq. (5) inequalities. The effective level density increases with J as does $\Delta\omega_{\text{mol}}$, because of the increase in size of the average coupling matrix element. The onset of the quasicontinuum will thus depend on J and K, with the energy onset being lower for higher J or K values. This variable onset must, in turn, affect the absorption behavior. There are experimental data consistent with this suggestion. It was observed in a supersonic beam of SF_6 that the width of the multiphoton excitation spectra and the number of photons absorbed decreased with increasing expansion pressure.[39] This observation was attributed to rotational cooling in the beam. The lower rotational levels, with higher energy onset for the quasicontinuum and narrower distribution of oscillator strength, are less efficient in absorbing photons.

E. Unimolecular reaction rate

The destruction of the K_a, K_c quantum number at moderate rotational excitation and a vibrational state density of $\sim$0.1 per cm^{-1} supports the conventional assumption that K is a statistical degree of freedom near the dissociation limit of molecules.[40] The formaldehyde molecule is used as an example for discussion here. ρ_v is calculated to be 7 per cm^{-1} [41] at the recently determined[42] $H_2CO \rightarrow H_2 + CO$ barrier height of 29 400 $\pm$ 700 cm^{-1}. At this energy, in addition to the much larger ρ_v, two factors affecting the magnitude of matrix elements between the basis levels are qualitatively different from the 8000 cm^{-1} region: the zero-order vibrational quantum numbers are much larger and the ΔV's between neighboring levels are also larger. The former would increase the matrix element magnitude while the latter would decrease it. The two opposite trends could result in comparable

average matrix elements in the low and high energy regions. Since the level spacing would be more than an order of magnitude smaller near the top of the dissociation barrier, rotation-vibration interaction should be much more prominent near dissociation. This estimate indicates that, in the evaluation of unimolecular reaction rates by the RRKM model,[40] J is the only invariant for adiabatic reactions and a $(2J + 1)/4$ degeneracy factor should be included in counting the molecular density of states. The effect of the rotational degeneracy factor on RRKM rate constants has been demonstrated in a recent calculation by Troe.[43]

Recently evidence for the participation of rotation in molecular dynamical processes has come from several sources. Several works have discussed rotational effects in radiationless transition rates of electronically excited states. In the laser induced fluorescence spectra of the S_1 $14^1 1^2$ state of benzene, Riedle, Neusser, and Schlag observed only $K_c = 0$ and some $K_c = J$ rotational lines.[44] b_{2u} vibrational states may couple through a-axis Coriolis interaction with b_{1u} states and through b-axis Coriolis interaction with e_{2u} states. b-axis rotation, with its larger rotational constant, is expected to be a more effective Coriolis mixing mechanism than c-axis rotation. It was argued that Coriolis interactions between $14^1 1^2$ and other specific basis states that promote the radiationless transition led to reduced fluorescence quantum yield and the disappearance of the $K_c \neq 0$ and $J \neq K_c$ lines.[44] Lim and co-workers also demonstrated through a rotational contour analysis of S_1 pyrimidine fluorescence that Coriolis interactions play an important role in intramolecular vibrational relaxation.[45] The same conclusion was drawn by McDonald and co-workers in their analysis of the dispersed IR fluorescence from the fundamental CH stretching levels of a large molecule excited by an IR laser.[46] Pratt and co-workers have shown that Coriolis coupling effects within the electronically excited pyrazine $^1B_{3u}$ state affect the intersystem crossing process.[47] Furthermore, there have been elegant double resonance studies of collision induced vibrational energy transfer rates which are enhanced by Coriolis perturbations.[48] These results all point to the importance of rotational effects in intramolecular dynamics and in the analysis of spectra of highly excited vibrational levels.

VI. SUMMARY

Three groups of vibrational levels between 7400 and 8600 cm^{-1} in the $\tilde{X}$ $^1A_1$ state of formaldehyde were studied by stimulated emission spectroscopy. Since a wide range of intermediate rotational levels could be used, we were able to examine the J and K_a dependence of the dispersion of intensity of the spectroscopically active vibrational basis state among many nearby rotation-vibration levels. In the absence of rotation, most $\tilde{A}$–$\tilde{X}$ transitions into a sparse manifold of Franck–Condon allowed vibrational levels could be definitively assigned a set of normal mode quantum numbers. This simple pattern evolved into many rotation-vibration lines at higher rotational quantum numbers. This mixing of a single spectroscopically active level into many vibrational states is a consequence of rotation-induced Coriolis forces. The observed densities of spectral lines within a 20 cm^{-1} range are three times as large as the calculated total vibrational density of states. This indicates that Coriolis coupling significantly degrades both vibrational and K_a quantum numbers. The reasonableness of this interpretation was confirmed qualitatively by a calculation of the Coriolis matrix elements among nearby vibrational levels in a harmonic normal mode basis. However, in order to account fully for the observed intensity distribution and the number of observed lines, it will be necessary to consider anharmonic interactions among the harmonic states.

These results suggest that complete K_a mixing is likely to occur near a dissociation barrier or limit. They also suggest that there will be a dependence on rotational quantum numbers of the onset of quasicontinuum behavior in infrared multiphoton excitation and a similar dependence in the inhomogeneous linewidth of high overtone vibrational bands. The possibility of using rotational excitation to control or design an eigenstate of desired photochemical properties should be considered. It is clear from these results that rotation promotes mixing of vibrational modes (IVR). Realistic theoretical evaluations of intramolecular vibrational dynamics cannot neglect rotational effects.

ACKNOWLEDGMENTS

This work was supported by a contract from the Air Force Office of Scientific Research (F49620-83-C-0010). Acknowledgment is made to the Donors of the Petroleum Research Fund, administered by the American Chemical Society, for support of HLD in this research.

APPENDIX

A normal mode analysis for $\tilde{X}$ $^1A_1$ H_2CO has been performed[49] and was reproduced using the computer program by Schachtschneider.[50] The equilibrium geometry is from Ref. 26 and the force constants from Ref. 49 even though one vibrational assignment on which the Ref. 49 analysis was based has proven to be incorrect.[8] The calculated normal mode frequencies agree exactly with those in Ref. 49. The resultant Coriolis constants and coefficients are listed in Table VI. In addition to these coefficients, which are needed to evaluate the vibrational parts of the Coriolis matrix elements, p_i and q_i in Table III are expressed in terms of creation and annihilation operators $a_i^\dagger$ and a_i:

$$q_i = (\hbar/4\pi c\omega_i)^{1/2}(a_i + a_i^\dagger), \tag{A1}$$

$$p_i = -i(\pi\hbar c\omega_i)^{1/2}(a_i - a_i^\dagger), \tag{A2}$$

where the effects of $a_i^\dagger$ and a_i on $|v\rangle = |\ldots, v_i, \ldots\rangle$ are

$$a_i|\ldots, v_i, \ldots\rangle = v_i^{1/2}|\ldots, v_i - 1, \ldots\rangle, \quad v_i \neq 0,$$

$$a_i^\dagger|\ldots, v_i, \ldots\rangle = (v_i + 1)^{1/2}|\ldots, v_i + 1, \ldots\rangle. \tag{A3}$$

[1] G. Hose and H. S. Taylor, J. Chem. Phys. **76,** 5356 (1982).
[2] For a recent example of Fermi mixing in formaldehyde, see B. Maessen and M. Wolfsberg, J. Chem. Phys. **80,** 4651 (1984).
[3] In a *rigid* asymmetric top the combination K_a, K_c (or alternatively τ) is a valid *label* for rotational energy levels, irrespective of the asymmetry. K_a has a simple *physical* significance only in the prolate rotor limit and K_c in the oblate rotor limit. When the asymmetry parameters are not at one of these limits, the expansion of the rotational wave function in a symmetric rotor basis will contain components of more than one K_a in the prolate basis (or more than one K_c in the oblate basis). The Coriolis-induced mixing referred to in this paragraph degrades the goodness of K_a (or τ) *both* as a label and as a physical quantity.
[4] D. W. Noid, M. L. Koszykowski, and R. A. Marcus, Annu. Rev. Phys. Chem. **32,** 267 (1981).
[5] C. Kittrell, E. Abramson, J. L. Kinsey, S. A. MacDonald, D. E. Reisner, R. W. Field, and D. H. Katayama, J. Chem. Phys. **75,** 2056 (1981); W. D. Lawrance and A. E. W. Knight, *ibid.* **76,** 5637 (1982); W. D. Lawrance and A. E. W. Knight, J. Phys. Chem. **87,** 389 (1983).
[6] P. H. Vaccaro, J. L. Kinsey, R. W. Field, and H. L. Dai, J. Chem. Phys. **78,** 3659 (1983).
[7] E. Abramson, R. W. Field, D. Imre, K. K. Innes, and J. L. Kinsey, J. Chem. Phys. **80,** 2298 (1984).
[8] D. E. Reisner, P. H. Vaccaro, C. Kittrell, R. W. Field, J. L. Kinsey, and H. L. Dai, J. Chem. Phys. **77,** 573 (1982); D. E. Reisner, H. L. Dai, J. L. Kinsey, and R. W. Field, *ibid.* **80,** 5968 (1984).
[9] The rotational assignments are based on an atlas provided by D. A. Ramsay. D. A. Ramsay and S. M. Till, Can. J. Phys. **57,** 1224 (1979).
[10] P. H. Vaccaro, H. L. Dai, J. L. Kinsey, and R. W. Field, J. Mol. Spectrosc. (in preparation).
[11] D. J. Clouthier and D. A. Ramsay, Annu. Rev. Phys. Chem. **34,** 31 (1983), and references therein.
[12] S. J. Strickler and R. J. Barnhart, J. Phys. Chem. **86,** 448 (1982).
[13] J. M. F. Van Dijk, M. J. H. Kemper, J. H. M. Kerp, and H. M. Buck, J. Chem. Phys. **69,** 2453 (1978).
[14] D. C. Moule and A. D. Walsh, Chem. Rev. **75,** 67 (1975), and references therein.
[15] K. Shibuya, R. A. Harger, and E. K. C. Lee, J. Chem. Phys. **69,** 751 (1978).
[16] N. Garland, E. C. Apel, and E. K. C. Lee, Chem. Phys. Lett. **95,** 209 (1983).
[17] The total collisional relaxation (self-quenching) rate for the $13_{1,12}$, 4^1 level of the $\tilde{A}$ state of formaldehyde was measured to be 1.10×10^8 s^{-1} $Torr^{-1}$; P. H. Vaccaro, R. L. Redington, J. Schmidt, J. L. Kinsey, and R. W. Field (unpublished results).
[18] H. H. Nielsen, Rev. Mod. Phys. **23,** 90 (1951).
[19] G. Amat, H. H. Nielsen, and G. Tarrago, *Rotation-Vibration of Polyatomic Molecules* (Marcel Dekker, New York, 1971).
[20] H. W. Kroto, *Molecular Rotation Spectra* (Wiley, New York, 1975), Chap. 3.
[21] G. Herzberg, *Molecular Spectra and Molecular Structure, Vol. III. Electronic Spectra and Electronic Structure of Polyatomic Molecules* (Van Nostrand, New York, 1966), p. 111.
[22] H. A. Jahn, Phys. Rev. **56,** 680 (1939).
[23] A. Sinha and J. L. Kinsey, J. Chem. Phys. **80,** 2029 (1984).
[24] S. M. Lederman, J. H. Runnels, and R. A. Marcus, J. Phys. Chem. **87,** 4364 (1983).
[25] M. Allegrini, J. W. C. Johns, and A. R. W. McKellar, J. Mol. Spectrosc. **67,** 476 (1977).
[26] J. L. Duncan, Mol. Phys. **28,** 1177 (1974).
[27] H. L. Dai, R. W. Field, and J. L. Kinsey, J. Chem. Phys. **82,** 2161 (1985).
[28] E. B. Stechel and E. J. Heller, Annu. Rev. Phys. Chem. **35,** 563 (1984).
[29] K. V. Reddy and M. J. Berry, Chem. Phys. Lett. **52,** 111 (1977); **66,** 223 (1979).
[30] D. W. Chandler, W. E. Farneth, and R. N. Zare, J. Chem. Phys. **77,** 4447 (1982).
[31] J. M. Jasinski, J. K. Frisoli, and C. B. Moore, J. Chem. Phys. **79,** 1301 (1983).
[32] R. G. Bray and M. J. Berry, J. Chem. Phys. **71,** 4909 (1979).
[33] D. F. Heller and S. Mukamel, J. Chem. Phys. **70,** 463 (1979).
[34] E. L. Sibert III, W. P. Reinhardt, and J. T. Hynes, J. Chem. Phys. **81,** 1115, 1135 (1984).
[35] N. Bloembergen, C. D. Cantrell, and D. M. Larsen, in *Tunable Lasers and Applications,* edited by A. Mooradian, T. Jaeger, and P. Stokseth (Springer, Berlin, 1976), p. 162.
[36] J. G. Black, E. Yablonovitch, N. Bloembergen, and S. Mukamel, Phys. Rev. Lett. **38,** 1131 (1977).
[37] J. G. Black, P. Kolodner, M. J. Shultz, E. Yablonovitch, and N. Bloembergen, Phys. Rev. A **19,** 704 (1979).
[38] M. Quack, J. Chem. Phys. **69,** 1282 (1978).
[39] D. Bassi, A. Boschetti, G. Scoles, M. Scotoni, and M. Zen, Chem. Phys. **71,** 239 (1981).
[40] W. H. Miller, J. Am. Chem. Soc. **101,** 6810 (1979).
[41] E. S. Yeung and C. B. Moore, J. Chem. Phys. **60,** 2139 (1974).
[42] H. L. Dai, P. H. Vaccaro, J. L. Kinsey, and R. W. Field (unpublished results).
[43] J. Troe, J. Phys. Chem. **88,** 4375 (1984).
[44] E. Riedle, H. J. Neusser, and E. W. Schlag, J. Phys. Chem. **86,** 4847 (1982).
[45] B. E. Forch, K. T. Chen, H. Salgusa, and E. C. Lim, J. Phys. Chem. **87,** 2280 (1983).
[46] G. M. Stewart, M. D. Ensminger, T. J. Kulp, R. S. Ruoff, and J. D. McDonald, J. Chem. Phys. **79,** 3190 (1983).
[47] Y. Matsumoto, L. H. Spangler, and D. W. Pratt, J. Chem. Phys. **80,** 5539 (1984).
[48] J. G. Haub and B. J. Orr, Chem. Phys. Lett. **107,** 162 (1984), and references therein.
[49] J. L. Duncan and P. D. Mallinson, Chem. Phys. Lett. **23,** 597 (1973).
[50] R. G. Snyder and J. H. Schachtschneider, J. Mol. Spectrosc. **30,** 290 (1969).